



Publishers of distinguished academic, scientific and professional journals

[Help](#) [Sitemap](#)

LOG IN

For Authors, Editors, Board Members

Username

.....

Remember me

[Forgotten?](#)

[Home](#) [For Authors](#) [Orders](#) [News](#)

International Journal of Environment and Waste Management (IJEWM)

Volume 8 - Issue 3/4 - 2011

Special Issue on Metal Ions Removal from Liquid Effluents: Part One


Guest Editor: Professor K.A. Matis

Table of Contents



Pages	Title and authors
215 - 228	<u>Two- and three-phase simulations of an ill-functioning dissolved-air flotation tank</u> <i>Vasiliki A. Emmanouil; Thodoris D. Karapantsios; Kostas A. Matis</i> DOI: 10.1504/IJEWM.2011.042632
229 - 240	<u>Removal of copper and lead ions from aqueous solutions by adsorbent derived from sewage sludge</u> <i>YunBo Zhai; GuangMing Zeng; LaFang Wang; XianXun Wei; CaiTing Li; ShanHong Li</i> DOI: 10.1504/IJEWM.2011.042633
241 - 257	<u>Removal of Pb²⁺ and Zn²⁺ ions from Acidic Soil Leachate: a comparative study between electrocoagulation, adsorption and</u>



- » [Objectives](#)
- » [Readership](#)
- » [Contents](#)
- » [Subject Coverage](#)
- » [Editorial Board](#)
- » [Specific Notes for Authors](#)
- » [Sample issue](#)
- » [Forthcoming Papers](#)
- »  [Latest TOC](#)

chemical precipitation processes*Patrick Drogui; Nathalie Meunier; Guy Mercier; Jean-Francois Blais*

DOI: 10.1504/IJEWM.2011.042634

258 - 272 **Batch sorption of lead (II) from aqueous solutions using natural kaolinite***Xue-Song Wang*

DOI: 10.1504/IJEWM.2011.042635

273 - 285 **A hybrid flotation: microfiltration cell for effluent treatment***Efrosyni N. Peleka; Nick K. Lazaridis; Kostas A. Matis*

DOI: 10.1504/IJEWM.2011.042636

286 - 304 **A critical review of the separation of arsenic oxyanions from dilute aqueous solution (the contribution of LGICT)***Eleni A. Deliyanni; Efrosini N. Peleka; George P. Gallios; Kostas A. Matis*

DOI: 10.1504/IJEWM.2011.042637

305 - 324 **Lariat ethers with a novel proton-ionisable groups: new generation of collectors in ion flotation process***Pawel Maciejewski; Malgorzata Ulewicz; Waldemar Robak; Wladyslaw Walkowiak*

DOI: 10.1504/IJEWM.2011.042638

325 - 340 **Cr(III) uptake by marine algal biomass: equilibrium and kinetics***Vitor J.P. Vilar; Olga M.M. Freitas; Pedro M.S. Costa; Cidalia M.S.**Botelho; Ramiro J.E. Martins; Rui A.R. Boaventura*

DOI: 10.1504/IJEWM.2011.042639

341 - 352 **Uptake of heavy metals from aqueous solution by non-conventional adsorbents***S.J. Patil; A.G. Bhole; G.S. Natarajan*

DOI: 10.1504/IJEWM.2011.042640

353 - 365 **Development of an on-site Fe⁰ system for treatment of copper- and zinc-contaminated roof runoff****Browse Recent Issues:**

» 2012 Vol.9 No. 3/4

» 2012 Vol.9 No. 1/2

» 2011 Vol.8 No. 3/4

» 2011 Vol.8 No. 1/2

» 2011 Vol.7 No. 3/4

» 2011 Vol.7 No. 1/2

» 2010 Vol.6 No. 3/4

» 2010 Vol.6 No. 1/2

» 2010 Vol.5 No. 3/4

» 2010 Vol.5 No. 1/2

» 2009 Vol.4 No. 3/4

» 2009 Vol.4 No. 1/2

» 2009 Vol.3 No. 3/4

» 2009 Vol.3 No. 1/2

» 2008 Vol.2 No. 6

» 2008 Vol.2 No. 4/5

» 2008 Vol.2 No. 3

» 2008 Vol.2 No. 1/2

» 2007 Vol.1 No. 4

» 2007 Vol.1 No. 2/3

» 2006 Vol.1 No. 1

R. Rangsviek; M.R. Jekel

DOI: 10.1504/IJEWM.2011.042641

366 - 382 [11 Å tobermorite ion exchanger from recycled container glass](#)

Nichola J. Coleman

DOI: 10.1504/IJEWM.2011.042642

383 - 403 [Nano-structured calcium silicate as sorbent in a study of artificial mining waste](#)

Thomas Borrmann; Mathew J. Cairns; Bradley G. Anderson; Wolfgang H. Holl; James H. Johnston

DOI: 10.1504/IJEWM.2011.042643

Pages Title and authors

1 **Cr(III) Uptake by Marine Algal Biomass: Equilibrium and Kinetics**

2
3 Vítor J. P. Vilar¹, Olga M.S. Freitas², Pedro M. S. Costa³, Cidália M. S. Botelho⁴, Ramiro J.E. Martins⁵,
4 Rui A. R. Boaventura^{6*}

5
6 ¹Pos-Doc Researcher, Laboratory of Separation and Reaction Engineering

7 Department of Chemical Engineering, Faculty of Engineering, University of Porto

8 Rua Dr. Roberto Frias, 4200-465 Porto, Portugal

9 E-mail: vilar@fe.up.pt

10
11 ²Assistant Professor, Department of Chemical Engineering,

12 School of Engineering SEP, Polytechnic Institute of Porto

13 Rua Dr. António Bernardino de Almeida, 431, 4200-072 Porto, Portugal

14 E-mail: omf@fe.up.pt

15
16 ³Chemical Engineer, Hydrological Quality Centre of the Health National Institute,

17 Dr. Ricardo Jorge, Largo 1º de Dezembro, 4049-019 Porto, Portugal

18 E-mail: pmsc@netcabo.pt

19
20 ⁴Auxiliar Professor, Laboratory of Separation and Reaction Engineering

21 Department of Chemical Engineering, Faculty of Engineering, University of Porto

22 Rua Dr. Roberto Frias, 4200-465 Porto, Portugal

23 E-mail: cbotelho@fe.up.pt

24
25 ⁵Assistant Professor, Department of Chemical and Biological Technology,

26 Polytechnic Institute of Bragança, Campus de Santa Apolónia,

27 Apartado 1134, 5301-857 Bragança, Portugal

28 E-mail: rmartins@ipb.pt

29 ⁶Principal Investigator, Laboratory of Separation and Reaction Engineering

30 Department of Chemical Engineering, Faculty of Engineering, University of Porto

31 Rua Dr. Roberto Frias, 4200-465 Porto, Portugal

32 E-mail: bventura@fe.up.pt

33 * Corresponding author

34 **Abstract**

35

36 In this work, biosorption of trivalent chromium by the marine brown algae *Sargassum muticum* was
37 studied in a batch system. The effect of the solution pH on Cr(III) uptake by *Sargassum* was
38 investigated. Kinetics and equilibrium experiments were conducted at different pH values (3.0, 4.0 and
39 5.0). Equilibrium data are well described by the Langmuir and Langmuir-Freundlich isotherms and
40 kinetics follows the pseudo-second-order model, at different pH values. The two mass transfer models
41 give comparable results, but they did not provide a perfect representation of the sorption data. The
42 homogeneous diffusivity, D_h , was found to be around $1.6 \times 10^{-8} \text{ cm}^2 \text{ s}^{-1}$ for 100 mg l^{-1} Cr(III)
43 concentration.

44 *Sargassum muticum* was compared with the brown algae *Laminaria hyperborean* and the red algae
45 *Gelidium sesquipedale* in terms of uptake capacity. The maximum uptake capacities for *Sargassum*,
46 *Laminaria* and *Gelidium* were, respectively, 56 ± 3 , 70 ± 4 and $18 \pm 1 \text{ mg Cr(III) g}^{-1}$, at pH = 5.

47

48 **Keywords:** *Sargassum*, *Gelidium*, *Laminaria*, Equilibrium, Kinetics, Marine Algae

49

50 **Reference** to this paper should be made as follows: Vilar, V.J.P., Freitas O.M.S., Costa, P.M.S.,
51 Botelho, C.M.S., Martins R.J.E. and Boaventura, R.A.R. (xxxx) 'Cr(III) Uptake by Marine Algal
52 Biomass: Equilibrium and Kinetics', *Int. J. Environment and Pollution*, Vol. X, No. Y., pp.000 000.

53

54 **Biographical notes:** Vítor Vilar received his graduation in Chemical Engineering from the University
55 of Porto, Portugal, in 2001, a PhD in Chemical Engineering from the same institution in 2006 and a
56 pos-graduation in Environmental Management. He is currently working as a research student in river
57 water quality simulation. He has authored 8 papers in international scientific periodicals with referees,
58 1 paper in an edited book, 6 papers in conference proceedings, 3 oral communications in international
59 conferences and 6 posters in national and international conferences. His specialization domain is on the
60 treatment of heavy metal contaminated waters by biosorption with low cost adsorbents, as algae, algal
61 waste and others; and his present research interests are on river water quality modeling and dye house
62 effluents detoxification using solar radiation.

63

64 Olga Freitas is an Assistant Professor in the Department of Chemical Engineering at the School of
65 Engineering SEP, Polytechnic Institute of Porto, Portugal. She is graduated in Chemical Engineering at
66 the Polytechnic Institute of Porto in 1996 and got a Master degree in Environmental Engineering at the
67 University of Porto in 2000. Currently she is finishing studies on heavy metals removal by biosorption
68 onto marine macro algae, in order to obtain a PhD degree in Chemical Engineering.

69

70 Pedro Costa received his graduation in Chemical Engineering from the University of Porto, in 2002,
71 with a specialization in Bioengineering, and a post-graduation in Environmental Engineering at the
72 University of Porto, in 2005. At the present he is working at the Hydrological Quality Centre of the
73 Health National Institute, Dr. Ricardo Jorge, in the area of water analysis.

74

75 Cidália Botelho is an Assistant Professor in the Department of Chemical Engineering at the University
76 of Porto, Portugal. She received her graduation in Chemical Engineering from the University of Porto,
77 in 1987, a master degree in applied Chemistry from the Technical University of Lisbon in 1992 and a
78 PhD in Chemical Engineering from University of Porto, in 1998. Her research interests are in
79 Environmental Chemistry and Engineering and also in the application of voltammetric techniques to
80 Environmental Analysis.

81

82 Ramiro Martins is an Assistant Professor in the Department of Chemical and Biological Technology at
83 the Polytechnic Institute of Bragança, Portugal. He received his graduation in Chemical Engineering
84 from the University of Porto, in 1991, a master degree in Environment Technology from the University
85 of Braga in 1995 and a PhD in Chemical Engineering from University of Porto, in 2004. His research
86 interests are in treatment of heavy metal contaminated waters by biosorption with low cost adsorbents,
87 biomonitoring of surface waters and environmental engineering. He also acts in the water and
88 wastewater market in a small company (design management and sales).

89

90 Rui Boaventura is a Principal Investigator in the Department of Chemical Engineering at the University
91 of Porto, Portugal. He received his graduation in Chemical Engineering from the University of Porto, in
92 1969 and a PhD in Chemical Engineering from University of Porto, in 1986. He has over 30 years of
93 experience in teaching, research and consulting in chemical and environmental engineering. His current

94 research interests include colour removal from textile wastewaters using low-cost adsorbents, heavy
95 metal removal from contaminated waters by biosorption, formation and fate of disinfection by-products
96 and biogeochemical transformations in surface waters. He has published about 40 papers in peer-
97 reviewed environmental journals and presented over 80 communications in international conferences.
98 He is member of the International Water Association.
99

100 Nomenclature

- 101
102 a_p specific area of thin plate particles (cm^{-1})
103 C_i and C_f initial and final metal concentrations in the solution (mg l^{-1})
104 C_{eq} residual metal concentration in solution (mg l^{-1})
105 $C_b(t)$ concentration of metal species in the liquid phase (mg metal l^{-1})
106 C_{b_0} initial metal concentration in the liquid phase (mg l^{-1})
107 D_h homogeneous diffusion coefficient inside the particle ($\text{cm}^2 \text{s}^{-1}$)
108 L half of the thin plate thickness (cm)
109 $k_{1,ads}$ biosorption constant of pseudo-first-order equation (min^{-1})
110 $k_{2,ads}$ biosorption constant of pseudo-second-order equation ($\text{min}^{-1} \text{g mg}^{-1}$).
111 K_L equilibrium constant for the Langmuir equation (l mg^{-1})
112 K_{LF} equilibrium constant for the Langmuir-Freundlich equation (l mg^{-1})
113 k_p mass transfer coefficient for intraparticle diffusion (cm s^{-1})
114 n empirical dimensionless parameter
115 q metal uptake (mg metal g^{-1} of the biosorbent)
116 q_{eq} amount of the metal adsorbed on the biosorbent at equilibrium (mg g^{-1})
117 q_L and q_{LF} maximum amount of metal per unit weight of biosorbent to form a complete monolayer on
118 the surface, respectively for Langmuir and Langmuir-Freundlich equation (mg g^{-1})
119 $\langle q(z,t) \rangle$ average metal concentration in the solid phase (mg g^{-1})
120 q_t concentration of metal in the sorbent at time t (mg g^{-1})
121 $r_{ads}(t)$ initial biosorption rate ($\text{mg g}^{-1} \text{min}^{-1}$)
122 V volume of solution (l)
123 $y_b(t)$ and $y(x,t)$ dimensionless metal concentrations in liquid and solid phase
124 $\langle y(x,t) \rangle$ dimensionless metal concentration inside the particle
125 y_{eq} dimensionless metal concentration in the solid phase
126 x dimensionless axial coordinate inside the particle
127 z distance to the symmetry plane (cm)
128 W dry weight of biosorbent (g)
129 ξ dimensionless factor for the batch capacity
130 τ_l particle diffusion time constant (s)

132 1 Introduction

133
134 Chromium main uses are in alloys, such as stainless steel, chrome plating leather tanning, and metal
135 ceramics. Chromium plating was once widely used to give steel a polished silvery mirror coating; it is
136 used in metallurgy to impart corrosion resistance and a shiny finish; as dyes and paints, its salts colour
137 glass an emerald green and it is used to produce synthetic rubies; to make moulds for the firing of
138 bricks (WHO, 1988).

139 Chromium(III) is an essential nutrient for humans and shortages may cause heart conditions,
140 disruptions of metabolisms and diabetes. But the uptake of too much chromium(III) can cause health
141 harmful effects as well, for instance skin rashes (WHO, 1988).

142 Chromium, and most trivalent chromium compounds, have been listed by the National Toxicology
143 Program (NTP) as having inadequate evidence for carcinogenicity in experimental animals, but a long-
144 term exposure to Cr(III) is known to cause allergic skin reactions and cancer (Lide, 2006).

145 Crops contain systems that arrange the chromium-uptake to be low enough not to cause any harm. But
146 when the amount of chromium in the soil rises, this can still lead to higher concentrations in crops.
147 Acidification of soil can also influence chromium uptake by crops (Lide, 2006).

148 Chromium is not known to accumulate in the bodies of fish, but high concentrations of chromium, due
149 to the disposal of metal bearing wastewaters in surface waters, can damage the gills of fish that swim

150 near the point of discharge. Chromium can cause respiratory problems in animals, a lower ability to
151 fight disease, birth defects, infertility and tumour formation (Lide, 2006).
152 In result of chromium toxicity, discharge limits have been regulated by most industrialized countries.
153 Conventional treatment of these effluents rich in chromium, as chemical precipitation,
154 oxidation/reduction, ion exchange and others, are extremely expensive (reagents consumption, safe
155 disposal of toxic sludge, technology) or inefficient for chromium removal from diluted solutions
156 (Volesky, 2003).
157 Nowadays, it has been confirmed that several low cost biological materials are able to effectively
158 remove chromium by sorption, as brown seaweed *Ecklonia sp.* (Yun et al., 2001), *Sargassum*
159 (Kratochvil et al., 1998), *Laminaria japonica* (Kang et al., 2004), blue-green algae *Spirulina sp.*
160 (Chojnacka et al., 2005), peat (Ma and Tobin, 2003), waste industrial *Mucor meihi* biomass (Tobin and
161 Roux, 1998), *Saccharomyces cerevisiae* residual cells from brewing industries (Ferraz et al., 2004), etc.
162 Metal uptake by biosorption is the result of a combination of different reactions that can occur in the
163 cell wall, as complexation, coordination and chelation of metals, ion exchange, adsorption and
164 microprecipitation (Volesky, 2003). The binding of chromium ions (Cr^{3+} and CrOH^{2+}) by protonated
165 brown alga *Ecklonia* biomass was attributed to carboxylic groups in the pH range 1-5, and the uptake
166 capacity increased with pH. An equilibrium model including the hydrolysis reactions that chromium
167 undergoes in the aquatic phase and the Cr^{3+} and Cr(OH)^{2+} reactions with the binding sites was able to
168 predict the equilibrium data (Yun et al., 2001). Carboxyl groups are acidic, so at low pH they will be
169 protonated and thereby become less available for binding metals, which explains why the uptake of
170 many metals increases with increasing pH (Crist et al., 1991).
171 Protonated or Ca-form *Sargassum* seaweed biomass bound up to 40 mg g⁻¹ of Cr(III) by ion exchange
172 at pH 4. An ion-exchange model assuming that only species taken up by the biomass was Cr(OH)^{2+}
173 successfully fitted the experimental biosorption data for Cr(III) (Kratochvil et al., 1998).
174 Waste industrial *Mucor meihi* biomass was found to be an effective biosorbent for the removal of
175 chromium from industrial tanning effluents. Sorption levels of 1.15 and 0.7 mmol g⁻¹ were observed at
176 pH 4 and 2, respectively. Acid elution of biosorbed chromium increased with decreasing eluant pH to a
177 maximum value of ca. 30% at pH near zero (Tobin and Roux, 1998).
178 Kinetic, equilibrium and dynamic (packed bed column) adsorption studies have been performed
179 successfully, using as adsorbate Pb(II), Cu(II), Cd(II) and Zn(II) ions, and the red algae *Gelidium*
180 *sesquipedale* as biosorbent (Vilar et al., 2006a, Vilar et al., 2006c, , 2007). The metal ion uptake was
181 attributed to the carboxylic groups present in the structure of the algae, determined by potentiometric
182 titration (Vilar, 2006). A continuous model, considering a heterogeneous Sips distribution of the
183 binding equilibrium constants fitted well the equilibrium experimental data (Vilar et al., 2006c). The
184 kinetic data in batch and continuous systems were also well described by a mass transfer model (Vilar
185 et al., 2006a, 2006b, Vilar et al., 2007).
186 Until now biosorption of trivalent chromium by algae *Sargassum muticum* has not been described.
187 Large quantities of these algae are available in the Portuguese coast and can be used for metal removal.
188 Ria Formosa, in the south of Portugal, has been invaded by *Sargassum muticum*, putting in danger the
189 ecosystem biodiversity. So, it's a matter of concern to remove this algal biomass, and find out an
190 interesting application for the large quantities available.

191 192 **2 Material and methods**

193 194 *2.1 Biosorbents*

195
196 The brown seaweeds *Sargassum muticum* and *Laminaria hyperborea* were collected along Portuguese
197 northern coast. The red algae *Gelidium sesquipedale* was harvested from central and southern coast.
198 The algae were washed with tap water and distilled water to remove most salts, air-dried during two
199 days to remove odours and most water and, after that, dried at 60°C and crushed in a mill. Algal
200 particles were then sieved (AS200 digit Retsch shaker) to obtain a fraction of 0.5-0.85 mm. The
201 equivalent length and width of the particles were about 2.5 mm and 0.6 mm, respectively, and thickness
202 0.1 mm.

203 204 *2.2 Chromium solutions*

205
206 Chromium(III) solutions were prepared by dissolving a weighted quantity of nonhydrated chromium
207 (III) nitrate (Carlo Erba, 98%) in distilled water. Solution pH values were controlled during kinetic and
208 equilibrium experiments to 5.0, 4.0 and 3.0 by addition of HNO₃ 0.01/0.1 M and NaOH 0.01/0.1 M
209 solutions.

210

211 2.3 Sorption kinetic studies

212

213 In order to determine the contact time required to reach equilibrium, biosorption dynamic experiments
214 were performed. Batch experiments were carried out in a 1-liter capacity glass vessel, equipped with a
215 cooling jacket (Grant type VFP) to ensure a constant 20 °C temperature during the experiment. The pH
216 was monitored and controlled with a WTW 538 pH/temperature meter. For kinetic experiments the
217 vessel was filled with 0.5 l of distilled water and a known weight of adsorbent was added. The
218 suspension was stirred for 10 min at 600 rpm stirring rate (magnetic stirrer Heidolph MR 3000) for
219 initial solution pH correction, and then the metal solution (0.5 l of a 200 mg l⁻¹ solution, which leads to
220 an initial concentration of 100 mg l⁻¹) was added maintaining the same stirring rate. 5 ml samples were
221 taken out at pre-determined time intervals ranging from 1 to 10 minutes after addition of the metal
222 solution. Samples were centrifuged (Eppendorf Centrifuge 5410) and the supernatant stored for Cr(III)
223 analysis.

224

225 2.4 Sorption equilibrium studies

226 The experiments were performed in duplicate, using 100 ml Erlenmeyer flasks, at pH = 5.0, 4.0 and
227 3.0 and temperature 20°C. The initial metal concentration was changed between 10 and 200 mg l⁻¹. A
228 given amount of biomass was suspended in 100 ml metal solution and stirred at 100 rpm. The solution
229 pH was adjusted by using 0.01 M NaOH and HCl solutions and temperature was maintained constant
230 (20°C) by using a HOTTECOLD thermostatic refrigerator. Once equilibrium was reached, samples
231 were taken out and centrifuged (Eppendorf Centrifuge 5410) for Cr(III) analysis in the supernatant.

232

233 2.5 Analytical procedure

234

235 Metal concentration was determined by atomic absorption spectrometry (GBC 932 Plus Atomic
236 Absorption Spectrometer). The amount of metal adsorbed per gram of biosorbent was calculated from
237 the metal mass balance.

238

239 3. Results and discussion

240

241 3.1 Equilibrium

242

243 Biosorption of Cr(III) ions by *Sargassum muticum* is highly pH dependent, as can be seen in Fig. 1.
244 The pH influences both metal binding sites on the cell surface and metal chemistry in solution.
245 According to the chromium speciation diagram in aqueous solution (Haug and Smidsrod, 1970), for
246 the pH range 1.5-5, the predominant Cr(III) species in solution are Cr³⁺ and Cr(OH)²⁺ (Cr(OH)⁺ also
247 exists at this pH range but in a very low concentration). For pH < 2.5, Cr(OH)²⁺ is no more present in
248 solution, and Cr³⁺ starts to precipitate as Cr(OH)₃ at pH > 5.0. Two major species, Cr³⁺ and Cr(OH)²⁺,
249 can bind with functional groups present on the surface of the biosorbent.

250

251 INSERT FIG.1

252

253 As the pH increases, the active sites, such as carboxyl and sulphate groups carry negative charges and
254 subsequently attract metal ions. So, biosorption onto cell surfaces increases. Yun et al. (2001) studied
255 the biosorption of trivalent chromium on brown alga *Ecklonia* biomass, and concluded that, even at pH
256 > 3.35, the contribution of Cr³⁺ binding to the chromium uptake was significant (identical
257 concentrations of Cr³⁺ and Cr(OH)²⁺ in aqueous phase), indicating that Cr³⁺ has higher affinity to the
258 binding sites than Cr(OH)²⁺.

259 Fig. 2 presents obtained equilibrium data for Cr(III) adsorption on algae *Sargassum muticum* at three
260 different pH (3.0, 4.0 and 5.0). Two equilibrium models were used to describe the equilibrium data:

261 Langmuir isotherm equation (Langmuir, 1918):

$$262 \quad q_{eq} = \frac{q_L K_L C_{eq}}{1 + K_L C_{eq}} \quad (1)$$

263 Langmuir-Freundlich (LF) isotherm, derived from the Langmuir and Freundlich models (Sips, 1948):

$$264 \quad q_{eq} = \frac{q_{LF} K_{LF} (C_{eq})^{(1/n)}}{1 + K_{LF} (C_{eq})^{(1/n)}} \quad (2)$$

where C_{eq} and q_{eq} represent the residual metal concentration in solution and the amount of the metal adsorbed on the biosorbent at equilibrium, respectively, q_L and q_{LF} are the maximum amount of metal per unit weight of biosorbent to form a complete monolayer on the surface, K_L is a coefficient related to the affinity between the sorbent and the metal ions, K_{LF} is the equilibrium constant, and n is an empirical dimensionless parameter.

INSERT FIG. 2

Experimental equilibrium data are well predicted by Langmuir and Langmuir-Freundlich adsorption isotherms. Model parameters, including statistical ones, are presented in Tables 1 and 2. No statistical difference was found between the two models, as given by the application of the test F for a 95% confidence level. So, results will be compared using Langmuir model.

INSERT TABLES 1 AND 2

Fig. 3 compares the adsorption behaviour of three different algae species, brown algae *Sargassum muticum* and *Laminaria hyperborea*, and red algae *Gelidium sesquipedale*, at pH = 5 and T = 20°C. Brown algae present a higher uptake capacity for chromium than red algae *Gelidium*, because they have more surface carboxyl groups (≈ 2.6 mmol g⁻¹) (Figueira et al., 2000, Lodeiro et al., 2005) when compared with algae *Gelidium* (≈ 0.36 mmol g⁻¹) (Vilar, 2006). Carboxyl groups are mainly due to alginic acid (brown algae) and agarose (*Gelidium*). The values of $q_L \times K_L$ presented in Table 1, indicate metal ions affinity for surface groups. Results show that metal ions bind with brown algae functional groups more easily than with algae *Gelidium*. Alga *Laminaria* is the best biosorbent as it can accumulate a greater amount of metal ions, principally for equilibrium concentrations higher than 20 mg l⁻¹.

INSERT FIG. 3

The adsorption of trivalent chromium ions has been studied, using different kinds of biosorbents: crab shell (*Chinonecetes opilio* obtained as waste from a crabmeat processing plant) ($q_L = 21$ mg g⁻¹, pH = 5.0, T = 30°C) (Kim, 2003), *Sargassum sp.* (Brazilian coast) ($q_L = 60$ mg g⁻¹, pH = 5.0, T = 30°C) (Cossich et al., 2002), a residue of *Sargassum sp.* seaweed obtained after extraction of biological cosmetics ($q_L = 300$ mg g⁻¹, pH = 6.0, T = 55°C) (Carmona et al., 2005), brown seaweed *Ecklonia sp.* (seashore of Pohang, Korea) ($q_L = 34$ mg g⁻¹, pH = 4, T = 20°C), algal biomass *spirogyra spp.* treated with 0.2 M CaCl₂ ($q_L = 30.21$ mg g⁻¹, pH = 5, T = 25°C) (Bishnoi et al., 2006), carrot residues ($q_L = 40$ mg g⁻¹, pH = 5.0, T = 25°C) (Nasernejad et al., 2005), bacterium *Pseudomonas aeruginosa* ($q_L = 7$ mg g⁻¹, pH not given, T = 25°C) (Kang et al., 2006), milled peat form supplied by Bord and Mona (Newbridge, Co. Kildare, Ireland) ($q_L = 21$ mg g⁻¹, pH = 5, T = 22-25°C) (Ma and Tobin, 2003), yeast *Candida tropicalis* ($q_L = 4.6$ mg g⁻¹) and filamentous bacterium *Streptomyces noursei* ($q_L = 1.8$ mg g⁻¹) (Mattuschka et al., 1993). These results show that the brown algae studied in this work are similar to the best biosorbents presented above, with respect to Cr(III) uptake capacity.

3.2 Kinetics

3.2.1 Kinetic models

Fig. 4 shows that biosorption is a fast process, occurring mainly in the first 40 minutes. The adsorption process takes place in two different stages: an initial and fastest stage, when high affinity and more accessible sites are occupied and a second stage that corresponds to the occupation of low affinity and more internal sites (Vilar, 2006).

INSERT FIG. 4 (a) AND (b)

In this work, two kinetic models were used (Lagergren, 1898, Ho and McKay, 1998):

Pseudo-first-order model

Pseudo-second-order model

$$q_t = q_{eq} [1 - \exp(-k_{1,ads} t)] \quad (3)$$

$$q_t = \frac{q_{eq}^2 k_{2,ads} t}{1 + k_{2,ads} q_{eq} t} \quad (4)$$

321 where q_t is the concentration of ionic species in the sorbent at time t (mg metal g^{-1} biosorbent), $k_{1,ads}$ is
 322 the biosorption constant of pseudo-first-order equation (min^{-1}) and $k_{2,ads}$ is the biosorption constant of
 323 pseudo-second-order equation ($min^{-1} g \text{ biosorbent } mg \text{ metal}^{-1}$).
 324 Kinetic data in Fig. 4 are fitted by the pseudo-first order and the pseudo-second order models. The
 325 performance of both models was compared by using the F Test, which let us to conclude that the
 326 pseudo-second-order model fits better the kinetic data for the three pH values (95% confidence level).
 327 Model parameters are presented in Tables 3 and 4. The values of q_{eq} confirm a stronger chromium
 328 uptake at high pH values, as it was concluded from the equilibrium experiments. The initial
 329 biosorption rate ($r_{ads}(i)$) was calculated as:

$$330 \quad r_{ads}(i) = k_{1,ads} q_{eq} \quad (5) \quad \text{and} \quad r_{ads}(i) = k_{2,ads} q_{eq}^2 \quad (6)$$

331 for the pseudo-first order and pseudo-second order models, respectively. The initial biosorption rate
 332 increases with pH due to the increase of the affinity of the metal ions to the binding sites.

334 INSERT TABLES 3 AND 4

336 3.2.2 Mass transfer models

337
 338 In order to describe the dynamics of the biosorption process two mass transfer models were developed,
 339 a homogeneous diffusion model and a linear driving force model, that can be solved analytically
 340 (Rodrigues, 1974). The following assumptions were considered: (i) - negligible external diffusion, for
 341 an adequate stirring rate (600 rpm); (ii) - sorption rate controlled by homogeneous diffusion inside the
 342 particle or linear driving force approximation (LDF); (iii) - isothermal process; (iv) - equilibrium
 343 between bound and soluble metal concentrations, as formulated by Langmuir isotherm; (v) - particles
 344 as uni-dimensional thin plates.

346 Homogeneous Diffusion Model

347 Mass conservation inside the particles gives:

$$348 \quad \frac{\partial y(x,t)}{\partial t} = \frac{1}{\tau_d} \frac{\partial^2 y(x,t)}{\partial x^2}, \quad \tau_d = \frac{L^2}{D_h} \quad (7)$$

349 where τ_d is the time constant for diffusion of ionic species into the particle (min), D_h is the
 350 homogeneous diffusion coefficient inside the particle ($cm^2 s^{-1}$), and L is half of the thin plate thickness
 351 (cm).

352 The initial and boundary conditions for Eq. (7) are:

$$353 \quad t=0 \quad y_b(0) = I \quad (8)$$

$$354 \quad 0 \leq x < L \quad y(x,0) = 0 \quad (9)$$

$$355 \quad x=0 \quad \frac{\partial y(x,t)}{\partial x} = 0 \quad \forall t \quad (10)$$

$$356 \quad x=L \quad \frac{\partial y(x,t)}{\partial t} = -\frac{\xi}{\tau_d} K_L C_{b_0} [I - y(x,t)]^2 \left[\frac{\partial y(x,t)}{\partial x} \right]_{x=L} \quad (11)$$

357 Dimensionless variables:

$$358 \quad x = \frac{z}{L}; \quad y_b(t) = \frac{C_b(t)}{C_{b_0}}; \quad y(x,t) = \frac{q(z,t)}{q_L};$$

$$359 \quad \langle y(x,t) \rangle = \frac{\langle q(z,t) \rangle}{q_L}; \quad y_{eq} = \frac{q_{eq}}{q_L}; \quad \xi = \frac{W q_L}{V C_{b_0}}$$

360 where V is the metal solution volume (l), W the mass of biosorbent (g), $C_b(t)$ and $\langle q(z,t) \rangle$ the
 361 concentration of metal species in the liquid phase (mg metal l^{-1}) and the average metal concentration in
 362 the solid phase (mg metal g^{-1} biosorbent), respectively, z the distance (cm) to the symmetry plane, x the
 363 dimensionless axial coordinate inside the particle, C_{b_0} the initial metal concentration in the liquid
 364 phase (mg metal l^{-1}), $y_b(t)$ and $y(x,t)$ the dimensionless metal concentrations in liquid and solid

365 phase, $\langle y(x,t) \rangle$ the average metal concentration inside the particle, y_{eq} the dimensionless metal
 366 concentration in the solid phase, given by the equilibrium law, and ξ the dimensionless factor for the
 367 batch capacity. A collocation on finite elements method was used to solve the nonlinear parabolic PDE
 368 with the initial and boundary conditions for each model equation (Madsen and Sincovec, 1979).

369
 370 Linear Driving Force (LDF)

371 If the average metal concentration inside the particle is used instead of a concentration profile, the
 372 following equations are obtained:

373 Kinetic law:

$$374 \quad \frac{d\langle y(t) \rangle}{dt} = k_p a_p [y_{eq} - \langle y(t) \rangle]; \quad a_p = \frac{I}{L} \quad (12)$$

375 where k_p is the mass transfer coefficient for intraparticle diffusion (cm s^{-1}) and a_p is the specific area of
 376 the thin plate particles (cm^{-1}).

377 Mass conservation in the fluid inside the closed vessel:

$$378 \quad \langle y(t) \rangle = \frac{I}{\xi} (I - y_b(t)) \quad (13)$$

379 Initial condition:

$$380 \quad t = 0 \quad y_b(t) = I \quad \langle y(t) \rangle = 0 \quad (14)$$

381 Substituting Eq. (13) and the dimensionless Langmuir equation in Eq. (12) the following expression is
 382 obtained, which can be solved analytically:

$$383 \quad \frac{I}{k_p a_p} \frac{d y_b(t)}{d t} + \left(\frac{\xi K_L C_{b_0}}{I + K_L C_{b_0} y_b(t)} + I \right) y_b(t) = I \quad (15)$$

384 For a parabolic profile inside the particle, $k_p a_p = 3 D_h / L^2 = 3 / \tau_d$, where $k_p a_p$ is the mass
 385 transfer intraparticle resistance (min^{-1}).

386 The mass transfer models, presented in this work, were solved for the operating parameters, resulting
 387 in the simulated curves presented in Figs. 5 (a) and (b). Both models adjust well the experimental data,
 388 confirming that the LDF approximation can be considered. Concentration profiles inside the particle
 389 for different values of dimensionless time (t/τ_p) are presented in Figure 6. It can be seen that the metal
 390 concentration inside the particle follows approximately a parabolic profile for low values of (t/τ_p) and a
 391 linear profile near the equilibrium. The average metal concentrations inside the particle given by the
 392 two models are initially very different, but as (t/τ_p) increases they become closer and equal at
 393 equilibrium.

394
 395 **INSERT FIG. 5 (a), (b) AND (c)**

396
 397 The values of the mass transfer intraparticle resistance, diffusion time and homogeneous diffusion
 398 coefficient are presented in Table 5. The thickness of the thin plates was determined by microscopic
 399 observation ($L = 0.05$ mm). D_h values are lower than the diffusivity of Cr^{3+} in water ($5.85 \times 10^{-6} \text{ cm}^2 \text{ s}^{-1}$),
 400 suggesting that a resistance to the diffusion process exists.

401 The kinetic rate for the pseudo-first-order equation is defined as $dq_t/dt = k_{1,ads}(q_{eq} - q_t)$. When
 402 compared with the kinetic law used in the LDF model (Eq. (12)), $k_{1,ads}$ has the same meaning that
 403 $k_p a_p$. As, both values are of the same order of magnitude, the assumed mechanism is validated.

404
 405 **INSERT TABLE 5**

406 5 Conclusion

407
 408
 409 Biosorption of Cr(III) ions by brown seaweed *Sargassum muticum* can be considered as an innovative
 410 and effective process, giving good performances. Equilibrium is well described by Langmuir and
 411 Langmuir-Freundlich models. The maximum uptake capacity was obtained for the highest pH within
 412 the study range (3.0- 5.0). Biosorption kinetics is fast and well represented by the pseudo-second order
 413 model. The LDF model can be considered as a simple model, with an analytical solution, to describe
 414 mass transfer resistance in the biosorption process.

415
416
417
418
419
420
421
422
423
424
425
426
427
428
429
430
431
432
433
434
435
436
437
438
439
440
441
442
443
444
445
446
447
448
449
450
451
452
453
454
455
456
457
458
459
460
461
462
463
464
465
466
467
468
469
470
471
472
473
474

Acknowledgements

Financial support by FCT and European Community through FEDER (project POCI/AMB/57616/2004) is gratefully acknowledged. The authors are grateful to FCT for V. Vilar's doctorate scholarship (SFRH/BD/7054/2001).

475

References

- 476 Bishnoi, N. R., Kumar, R., Kumar, S. and Rani, S. (2006) 'Biosorption of Cr(III) from aqueous solution
477 using algal biomass *Spirogyra spp*', *J. Hazard. Mater.*, doi:10.1016/j.jhazmat.2006.10.093.
- 478 Carmona, M. E. R., da Silva, M. A. P. and Ferreira Leite, S. G. (2005) 'Biosorption of chromium using
479 factorial experimental design', *Proc. Biochem.*, Vol. 40, Nos. 2, pp. 779-788.
- 480 Chojnacka, K., Chojnacki, A. and Górecka, H. (2005) 'Biosorption of Cr³⁺, Cd²⁺ and Cu²⁺ ions by blue-
481 green algae *Spirulina sp.*: Kinetics, equilibrium and the mechanism of the process',
482 *Chemosphere*, Vol. 59, pp. 75-84.
- 483 Cossich, E. S., Tavares, C. R. G. and Ravagnani, T. M. K. (2002) 'Biosorption of chromium(III) by
484 *Sargassum sp.* Biomass', *Proc. Biotech.*, Vol. 5, Nos. 2, pp.
- 485 Crist, R. H., Martin, J. R. and Crist, D. R. (1991) 'Interaction of metals and protons with algae.
486 Equilibrium constants and ionic mechanisms for heavy metal removal as sulfides and
487 hydroxides', *Miner. Bioproc.*, pp. 275-287.
- 488 Ferraz, A. I., Tavares, T. and Teixeira, J. A. (2004) 'Cr(III) removal and recovery from *Saccharomyces*
489 *Cerevisiae*', *Chem. Eng. J.*, Vol. 105, pp. 11-20.
- 490 Figueira, M. M., Volesky, B., Ciminelli, V. S. T. and Roddick, F. A. (2000) 'Biosorption of metals in
491 brown seaweed biomass', *Water Res.*, Vol. 34, Nos. 1, pp. 196-204.
- 492 Haug, A. and Smidsrod, O. (1970) 'Selectivity of some anionic polymers for divalent metal ions', *Acta*
493 *Chem. Scand.*, Vol. 24, pp. 843-854.
- 494 Ho, Y. S. and McKay, G. (1998) 'Sorption of dye from aqueous solution by peat', *Chem. Eng. J.*, Vol.
495 70, pp. 115-124.
- 496 Kang, S.-Y., Lee, J.-U. and Kim, K.-W. (2006) 'Biosorption of Cr(III) and Cr(VI) onto the cell surface
497 of *Pseudomonas Aeruginosa*', *Biochem. Eng. J.*, doi:10.1016/j.bej.2006.06.005.
- 498 Kang, S.-Y., Lee, J.-U., Moon, S.-H. and Kim, K.-W. (2004) 'Competitive adsorption characteristics of
499 Co²⁺, Ni²⁺, and Cr³⁺ by IRN-77 cation exchange resin in synthesized wastewater',
500 *Chemosphere*, Vol. 56, pp. 141-147.
- 501 Kim, D. S. (2003) 'The removal by crab shell of mixed heavy metal ions in aqueous solution', *Biores.*
502 *Technol.*, Vol. 87, pp. 355-357.
- 503 Kratochvil, D., Pimentel, P. and Volesky, B. (1998) 'Removal of trivalent and hexavalent chromium by
504 seaweed biosorbent', *Environ. Sci. Technol.*, Vol. 32, pp. 2693-2698.
- 505 Lagergren, S. (1898) 'About the theory of so-called adsorption of soluble substances', *K. Sven.*
506 *Vetenskapsakad.*, Vol. Handlingar, Band 24, Nos. 4, pp. 1-39.
- 507 Langmuir, I. (1918) 'The adsorption of gases on plane surfaces of glass, mica and platinum', *J. Am.*
508 *Chem. Soc.*, Vol. 40, pp. 1361-1403.
- 509 Lide, D. R. (2006) *Handbook of Chemistry and Physics*. CRC press.
- 510 Lodeiro, P., Rey-Castro, C., Barriada, J. L., Vicente, M. E. S. d. and Herrero, R. (2005) 'Biosorption of
511 cadmium by the protonated macroalga *Sargassum muticum*: Binding analysis with a nonideal,
512 competitive, and thermodynamically consistent adsorption (NICCA) model', *J. Colloid*
513 *Interface Sci.*, Vol. 289, pp. 352-358.
- 514 Ma, W. and Tobin, J. M. (2003) 'Development of multimetal binding model and application to binary
515 metal biosorption onto peat biomass', *Water Res.*, Vol. 37, pp. 3967-3977.
- 516 Madsen, N. and Sincovec, R. (1979) 'PDECOL: General collocation software for partial differential
517 equations', *ACM Trans. Math. Soft.*, Vol. 5, Nos. 3, pp. 326-351.
- 518 Mattuschka, B., Junghaus, K. and Straube, G. (Eds.) (1993) *Biosorption of Metals by Waste Biomass*,
519 Warrendale, PA, The Minerals, Metals & Materials Society.
- 520 Nasernejad, B., Zadeh, T. E., Pour, B. B., Bygi, M. E. and Zamani, A. (2005) 'Camparison for
521 biosorption modeling of heavy metals (Cr (III), Cu (II), Zn (II)) adsorption from wastewater
522 by carrot residues', *Proc. Biochem.*, Vol. 40, pp. 1319-1322.
- 523 Rodrigues, A. E. (1974) Elementos sobre a Teoria de Percolação, Luanda, Universidade de Luanda,
524 Departamento de Engenharia Química.
- 525 Sips, R. (1948) 'On the structure of a catalyst surface', *J. Chem. Phys.*, Vol. 16, pp. 490-495.
- 526 Tobin, J. M. and Roux, J. C. (1998) 'Mucor biosorbent for chromium removal from tanning effluent',
527 *Water Res.*, Vol. 32, Nos. 5, pp. 1407-1416.
- 528 Vilar, V., Botelho, C. and Boaventura, R. (Eds.) (2006a) *Biosorption performance of a binary metal*
529 *mixture by algal biomass: Column experiments*, Kiev, Springer.
- 530 Vilar, V., Botelho, C. and Boaventura, R. (2006b) 'Continuous-flow metal biosorption in a regenerable
531 *Gelidium* column', *Revista Cubana de Química*, Vol. XVIII, Nos. 1.
- 532 Vilar, V. J. P. (2006) Remoção de iões metálicos em solução aquosa por resíduos da indústria de
533 extracção do agar, Ph.D. Thesis, *Chemical Engineering Department*. Porto, Faculty of
534 Engineering University of Porto.

535 Vilar, V. J. P., Botelho, C. M. S. and Boaventura, R. A. R. (2006c) 'Kinetics and equilibrium modelling
536 of lead uptake by algae *Gelidium* and algal waste from agar extraction industry', *J. Hazard.*
537 *Mater.*, Vol. 143, Nos. 1-2, pp. 396-408.
538 Vilar, V. J. P., Botelho, C. M. S. and Boaventura, R. A. R. (2007) 'Copper removal by algae *gelidium*,
539 agar extraction algal waste and granulated algal waste: Kinetics and equilibrium', *Biores.*
540 *Technol.*, doi:10.1016/j.biortech.2007.01.042.
541 Volesky, B. (2003) *Sorption and Biosorption*. Quebec, BV Sorbex, Inc.
542 WHO (1988) Environmental health criteria 61: Chromium, Geneva.
543 Yun, Y.-S., Park, D., Park, J. M. and Volesky, B. (2001) 'Biosorption of trivalent chromium on the
544 brown seaweed biomass', *Environ. Sci. Technol.*, Vol. 35, pp. 4353-4358.
545
546
547
548
549
550
551
552
553
554
555
556
557
558
559
560
561
562
563
564
565
566
567
568
569
570
571
572
573
574
575
576
577
578
579
580
581
582
583
584
585
586
587
588
589
590
591
592
593
594

List of Tables

595

596

597 **Table 1.** Estimated Langmuir equilibrium model parameters (value \pm standard deviation).

598

599 **Table 2.** Estimated Langmuir-Freundlich equilibrium model parameters (value \pm standard deviation).

600

601 **Table 3.** Estimated pseudo-first order model parameters (value \pm standard deviation).

602

603 **Table 4.** Estimated pseudo-second order model parameters (value \pm standard deviation).

604

605 **Table 5.** Estimated parameters for the linear driving force (LDF) and homogeneous particle diffusion
606 models.

607

608

609

610

611

612

613

614

615

616

617

618

619

620

621

622

623

624

625

626
627

Table 1. Estimated Langmuir equilibrium model parameters (value \pm standard deviation).

Biosorbent	pH	Langmuir model			R^2	S_R^2 (mg g^{-1}) ²	F_{cal}	$F_{1-\alpha}$
		q_L (mg g^{-1})	K_L (l mg^{-1}) $\times 10^2$	$q_L \times K_L$ (l g^{-1})				
<i>Sargassum</i>	5.0	56 ± 3	6 ± 1	3.4 ± 0.6	0.960	11.2	1.1	2.2
	4.0	33 ± 1	12 ± 1	3.9 ± 0.3	0.982	2.07	1.1	2.2
	3.0	19 ± 1	9 ± 1	1.7 ± 0.2	0.987	0.41	1.2	2.2
<i>Laminaria</i>	5.0	70 ± 4	4.2 ± 0.6	2.9 ± 0.6	0.971	12.9	1.9	2.1
<i>Gelidium</i>	5.3	18 ± 1	2.1 ± 0.4	0.38 ± 0.08	0.933	1.38	1.1	2.3

628
629
630
631
632
633
634
635
636
637
638
639
640
641
642
643
644
645
646
647
648
649
650
651
652
653
654
655
656
657
658
659
660
661
662
663
664
665
666
667
668
669
670
671
672
673
674

675
676

Table 2. Estimated Langmuir-Freundlich equilibrium model parameters (value \pm standard deviation).

Biosorbent	pH	Langmuir-Freundlich model			R^2	S_R^2 (mg g^{-1}) ²
		q_{LF} (mg g^{-1})	K_{LF} (1 mg^{-1}) $\times 10^2$	n		
<i>Sargassum</i>	5.0	50 ± 4	4 ± 1	0.8 ± 0.1	0.963	10.5
	4.0	32 ± 1	9 ± 2	0.85 ± 0.08	0.984	1.90
	3.0	22 ± 3	11 ± 2	1.3 ± 0.2	0.992	0.34
<i>Laminaria</i>	5.0	54 ± 2	1.1 ± 0.5	0.57 ± 0.06	0.984	6.66
<i>Gelidium</i>	5.3	25 ± 9	3.5 ± 0.9	1.4 ± 0.3	0.941	1.23

677
678
679
680
681
682
683
684
685
686
687
688
689
690
691
692
693
694
695
696
697
698
699
700
701
702
703
704
705
706
707
708
709
710
711
712
713
714
715
716
717
718
719
720
721
722

723
724

Table 3. Estimated pseudo-first order model parameters (value \pm standard deviation).

Biosorbent	pH	C_i (mg l ⁻¹)	Pseudo-first order model					F_{cal}	$F_{1-\alpha}$
			q_{eq} (mg g ⁻¹)	$k_{1,ads}$ (min ⁻¹)	R^2	S_R^2 (mg g ⁻¹) ²	$r_{ads(i)}$ (mg g ⁻¹ min ⁻¹)		
<i>Sargassum</i>	5.0	102	29.6 \pm 0.9	0.20 \pm 0.04	0.918	8.15	6 \pm 1	3.7	2.4
	4.0	109	24.7 \pm 0.6	0.22 \pm 0.03	0.932	3.85	5.4 \pm 0.8	3.1	2.3
	3.0	104	14.7 \pm 0.3	0.16 \pm 0.01	0.975	0.62	2.4 \pm 0.2	2.7	2.3

725

726

727

728

729

730

731

732

733

734

735

736

737

738

739

740

741

742

743

744

745

746

747

748

749

750

751

752

753

754

755

756

757

758

759

760

761

762

763

764

765

766

767

768

769

770

771

772

773
774

Table 4. Estimated pseudo-second order model parameters (value \pm standard deviation).

Biosorbent	pH	C_i (mg l ⁻¹)	Pseudo-second order model				
			q_{eq} (mg g ⁻¹)	$k_{2,ads}$ (g mg ⁻¹ min ⁻¹) $\times 10^2$	R^2	s_R^2 (mg g ⁻¹) ²	$r_{ads(i)}$ (mg g ⁻¹ min ⁻¹)
<i>Sargassum</i>	5.0	102	31.9 \pm 0.6	0.9 \pm 0.1	0.977	2.21	9 \pm 1
	4.0	109	26.1 \pm 0.4	1.5 \pm 0.2	0.977	1.23	10 \pm 1
	3.0	104	15.9 \pm 0.2	1.4 \pm 0.1	0.991	0.23	3.5 \pm 0.3

775
776
777
778
779
780
781
782
783
784
785
786
787
788
789
790
791
792
793
794
795
796
797
798
799
800
801
802
803
804
805
806
807
808
809
810
811
812
813
814
815
816
817
818
819
820
821
822

823 **Table 5.** Estimated parameters for the linear driving force (LDF) and homogeneous particle diffusion
 824 models.
 825

Biosorbent	C_i (mg l ⁻¹)	pH	LDF model			Homogeneous diffusion model			
			$k_p \times a_p$ (min ⁻¹)	τ_d (min)	S_R^2 (mg g ⁻¹) ²	τ_d (min)	D_h (cm ² s ⁻¹)	S_R^2 (mg g ⁻¹) ²	D_h (average) (cm ² s ⁻¹)
	102	5.0	0.12	25	15.9	25	1.7×10 ⁻⁸	11.5	
<i>Sargassum</i>	109	4.0	0.12	25	6.7	25	1.7×10 ⁻⁸	3.7	1.6×10 ⁻⁸
	104	3.0	0.11	27	1.0	27	1.5×10 ⁻⁸	0.5	

826

827

828

829

830

831

832

833

834

835

836

837

838

839

840

841

842

843

844

845

List of Figures

846
847
848
849
850
851
852
853
854
855
856
857
858
859
860
861
862
863
864
865
866
867

868

869

870

871

872

873

874

875

876

877

878

879

880

881

882

Figure 1. Influence of pH on the uptake capacity of Cr(III) by the algae *Sargassum muticum*.

Figure 2. Langmuir and LF isotherms for Cr(III) biosorption on the algae *Sargassum* at different pH (average $q_{eq} \pm$ standard deviation).

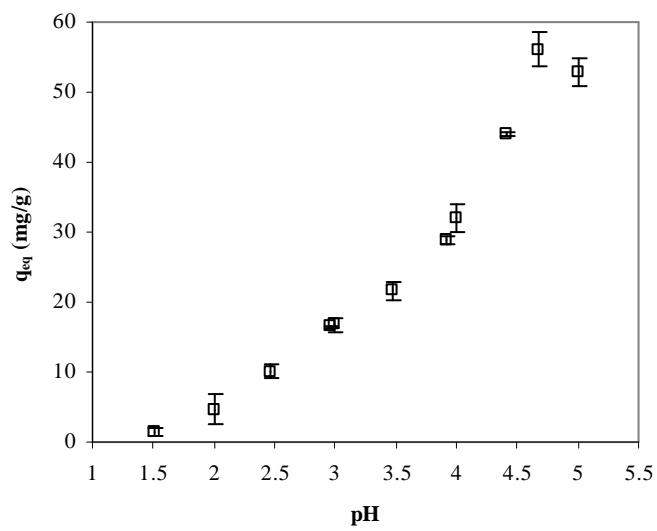
Figure 3. Comparison of the uptake capacity of three different species of algae and Langmuir and LF fit curves (average $q_{eq} \pm$ standard deviation).

Figure 4. Evolution of adsorbed Cr(III) on the algae *Sargassum* with contact time at different pH: experimental data and kinetic model curves.

Figure 5. Evolution of the dimensionless concentration in solution (a) and adsorbed Cr(III) concentration (b) on the algae *Sargassum* with contact time, at different pH: experimental data and mass transfer model curves (— Homogeneous diffusion model; --- Linear driving force model).

Figure 6. Concentration profiles inside the particle for different values of t/τ_d . Cr(III) concentration (y) predicted by the homogeneous particle diffusion model (—) and average metal concentration inside the particle predicted by the linear driving force model (---) and homogeneous diffusion model (- - -). (a) pH = 5.0, (b) pH = 4.0 and (c) pH = 3.0.

883 **Figure 1.**



884

885

886

887

888

889

890

891

892

893

894

895

896

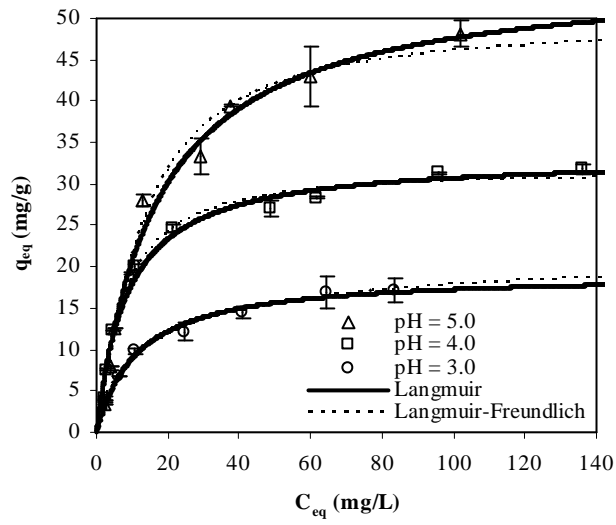
897

898

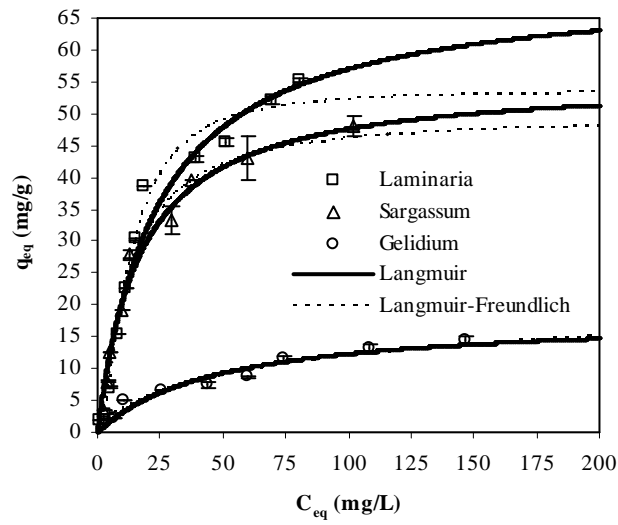
899

900

901 **Figure 2.**



919 **Figure 3.**



920

921

922

923

924

925

926

927

928

929

930

931

932

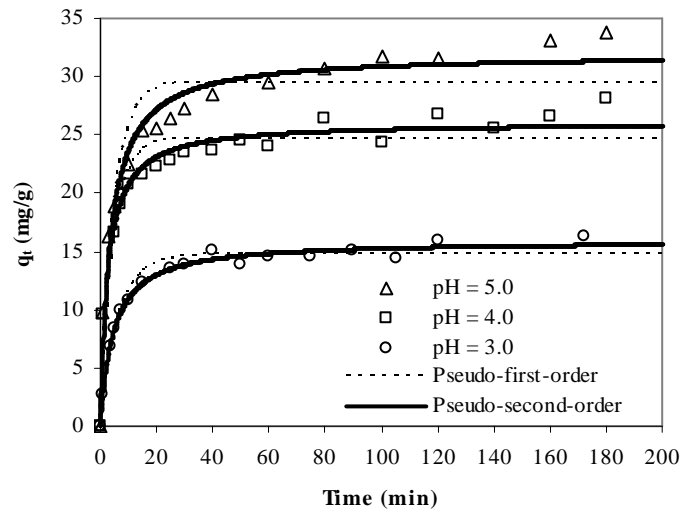
933

934

935

936

937 **Figure 4.**



938

939

940

941

942

943

944

945

946

947

948

949

950

951

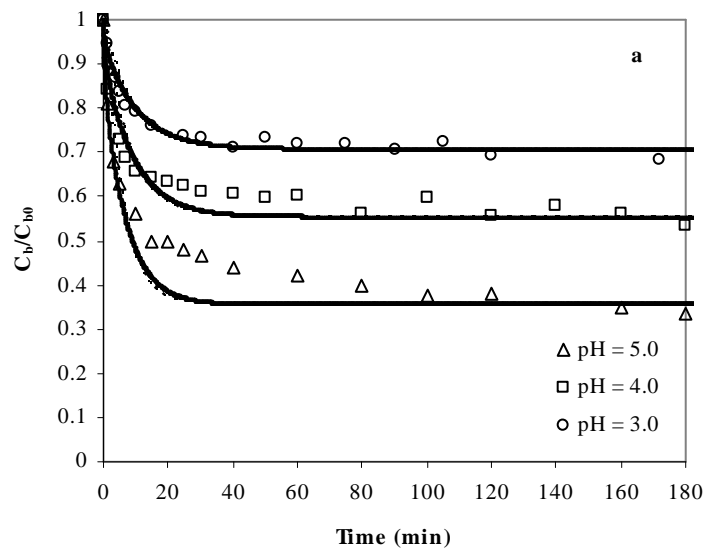
952

953

954

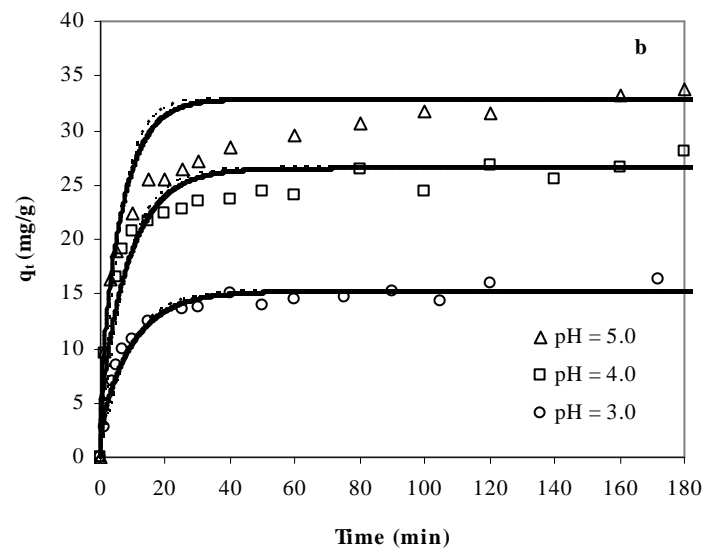
955 **Figure 5.**

956 **(a)**



957

958 **(b)**



959

960

961

962

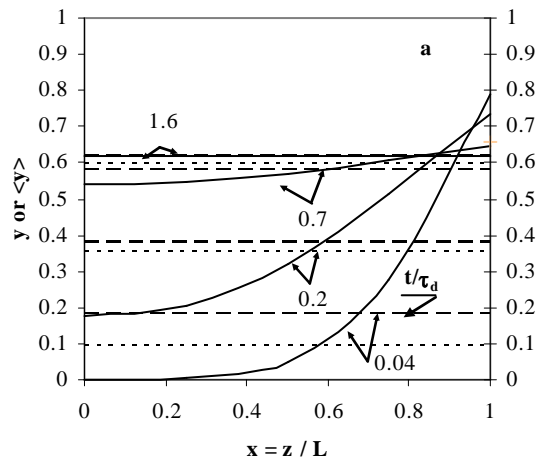
963

964

965

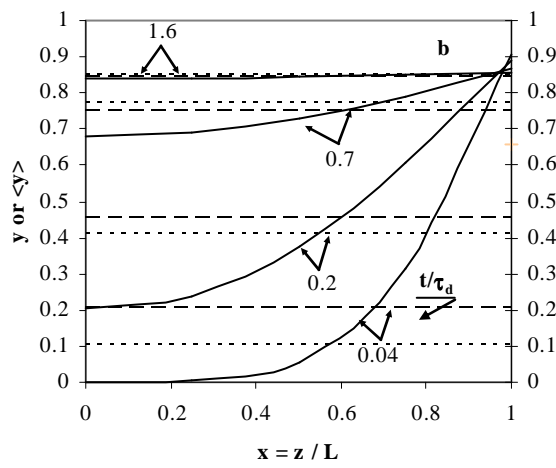
966 **Figure 6.**

967 **(a)**



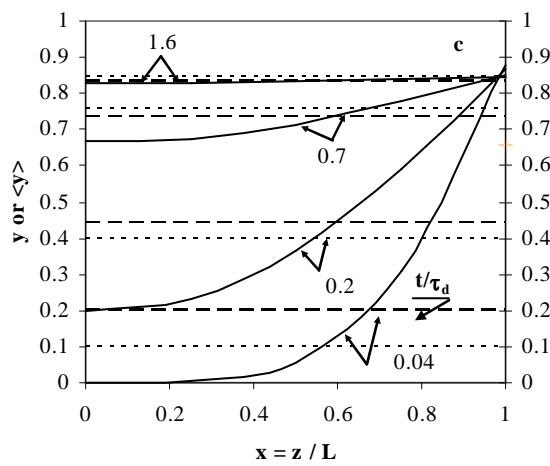
968

969 **(b)**



970

971 **(c)**



972